Tetrahedron 65 (2009) 7038–7047

Contents lists available at ScienceDirect

Tetrahedron

journal homepage: www.elsevier.com/locate/tet

Metal ion complexation in acetonitrile by upper-rim allyl-substituted, di-ionized calix[4]arenes bearing two dansyl fluorophores

Ümmühan Ocak [b,*], Miraç Ocak [b], Kazimierz Surowiec [a], Xiaodong Liu [a], Richard A. Bartsch [a]

[a] Department of Chemistry and Biochemistry, Texas Tech University, Lubbock, TX 79409-1061, USA
[b] Department of Chemistry, Faculty of Arts and Sciences, Karadeniz Technical University, 61080 Trabzon, Turkey

ARTICLE INFO

Article history:
Received 8 April 2009
Received in revised form 25 May 2009
Accepted 11 June 2009
Available online 17 June 2009

Keywords:
Calixarene ligand
Fluorescence spectroscopy
Stability constant
Metal ion complexation

ABSTRACT

The influence of Li^+, Na^+, K^+, Rb^+, Cs^+, Mg^{2+}, Ca^{2+}, Sr^{2+}, Ba^{2+}, Ag^+, Cd^{2+}, Co^{2+}, Fe^{2+}, Hg^{2+}, Mn^{2+}, Pb^{2+}, Zn^{2+} and Fe^{3+} on the spectroscopic properties of two dansyl (1-dimethylaminonaphthalene-5-sulfonyl) groups linked to the lower rims of a series of three, structurally related, di-ionized calix[4]arenes is investigated by means of absorption and emission spectrophotometry. Di(tetramethylammonium) salts of the di-ionized ligands, **L**, **L1**, and **L2**, which differ in having no, two and four allyl groups, respectively, on the upper rim of the calix[4]arene scaffold, are utilized for the spectrofluorimetric titration experiments in MeCN. On complexation by alkaline earth metal cations, the emission spectra undergo marked red shifts and quenching of the dansyl fluorescence. These effects are weaker with alkali metal cations. Transition metal cations and Pb^{2+} interact strongly with the ligands. In particular, Fe^{3+}, Hg^{2+} and Pb^{2+} cause greater than 99% quenching of the dansyl fluorescence.

1. Introduction

Fluorescent chemosensors are typically composed of a signal transducer (fluorophore) and a selective recognition unit (ionophore).[1–5] Macrocycles that possess ionophore ability have been used as recognition moieties in such molecular structures. The signaling moiety is responsible for the changes in the photophysical characteristics of the fluorophore. These changes may be photoinduced processes, such as electron transfer, charge transfer, energy transfer, and excimer or exciplex formation or disappearance.

Due to their ability to form complexes with metal ions, calixarenes have been used as recognition moieties in fluorescent chemosensors.[6–10] Various chemosensors based on calix[4]arenes bearing fluorescent groups have been synthesized for investigation of their fluorescent responses upon complexation with various metal cations.[11–15] Recently, dansyl and its derivatives have been generally used as fluorescent groups on chemosensors for metal detection and determination.[16–18] Depending upon the identity of substituents, calix[4]arene compounds may be conformationally mobile or restricted to cone, partial cone, 1,3-alternate or 1,2-alternate conformations. The ligand conformation may be important in metal complexation with calix[4]arenes.[19] Also substitution on the upper or lower rims may influence a metal ion complexation process. The complex may form due to hydrogen bonding, hydrophobic bonding or the electron donor–acceptor interactions.

Recently, Bartsch and co-workers have focused attention on the preparation of conformationally mobile or restricted di-ionizable calix[4]arenes for use in metal ion separations.[20–22] In some instances, dansyl fluorophores were incorporated into these structures for possible investigation of the complexation properties of such calix[4]arenes by solution fluorescence spectroscopy.

In an earlier study, we reported the interactions of didansyl-pendant, di-ionized calix[4]arenes with no, two and four *tert*-butyl groups on the upper rim (Fig. 1) with a variety of metal cation

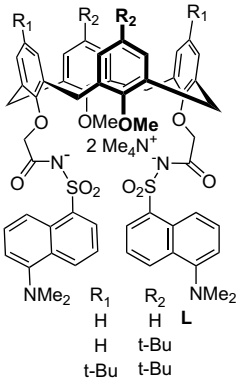

Figure 1. Structures of previously examined[23] di-ionized, didansyl calix[4]arene ligands.

* Corresponding author. Tel.: +90 462 377 25 96; fax: +90 462 325 31 96.
E-mail address: uocak@ktu.edu.tr (Ü. Ocak).

0040-4020/$ – see front matter © 2009 Elsevier Ltd. All rights reserved.
doi:10.1016/j.tet.2009.06.038

species using spectrophotometric and spectrofluorimetric techniques.[23] In this present paper, we report the synthesis of two novel calix[4]arene ligands with dansyl pendant groups on the lower rim and allyl groups on the upper rim and complexation properties of their di-ionized forms **L1** and **L2** (Fig. 2) with metal cations. The structures of ligands **1** and **2** differ in having two and four allyl groups on the upper rim of the calix[4]arene scaffold. Compared with the earlier investigated upper-rim *tert*-butyl groups in the ligand series shown in Figure 1, upper-rim allyl groups are less bulky but provide π bonds as potential interaction sites for metal ions. Responses of di(tetramethylammonium) salts of the di-ionizable ligands **L1** and **L2** to a variety of metal cations are assessed by spectrofluorometric titration in MeCN. Changes in the fluorescence spectra of **L1** and **L2** in the presence of various metal cations are compared with those reported earlier for **L**, an analog with no allyl groups on the upper rim. Stability constants and compositions of complexes of Hg^{2+}, Pb^{2+} and Fe^{3+} with **L1** and **L2** are determined. A Stern–Volmer approach is utilized to probe the quenching mechanism.

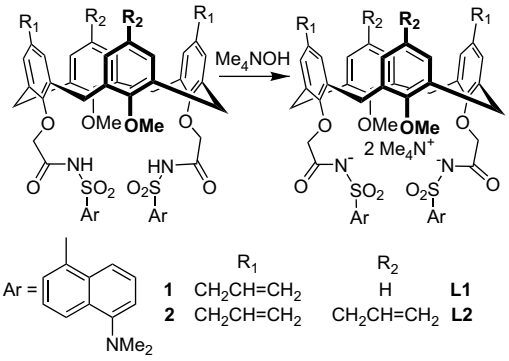

Figure 2. Structures of new didansyl calix[4]arene ionophores **1** and **2** and their di-ionized tetramethylammonium salts **L1** and **L2**, respectively.

2. Results and discussion

2.1. Synthetic routes

The syntheses of new di-dansylated, di-ionizable calix[4]arene ligands **1** and **2** are summarized in Schemes 1 and 2, respectively.

For the preparation of ligand **1** with two allyl groups on the upper rim of the calix[4]arene scaffold (Scheme 1), two methyl groups were attached to distal hydroxyl groups of calix[4]arene (**3**) to give known diether **4**, which underwent diallylation of the remaining phenolic units to produce reported tetraether **5**. Claisen rearrangement of **5** gave known diether **6** with an allyl group on the *para* position of each phenolic unit. Dialkylation of **6** with NaH and ethyl bromoacetate in THF provided an 88% yield of diester **7**. Basic hydrolysis of **7** with Me_4NOH in aq THF gave di(carboxylic acid) **8** in 99% yield. Reaction of diacid **8** with oxalyl chloride in C_6H_6 produced the corresponding di(acid chloride). Addition of the crude di(acid chloride) to a mixture of NaH and dansylamide in THF formed ligand **1** in 76% yield.

For the synthesis of ligand **2** with four allyl groups attached to the upper rim of the calix[4]arene scaffold (Scheme 2), calix[4]arene (**3**) was reacted with NaH and allyl bromide in THF/DMF to afford a 74% yield of known tetraether **9**. Claisen rearrangement of **9** gave reported upper-rim tetra-allylated calix[4]arene **10**. Compound **10** was reacted with NaH and MeOTs in MeCN to produce a 90% yield of distal diether **11**. Reaction of **11** with NaH and ethyl bromoacetate in THF gave diester **12** in 78% yield. Basic hydrolysis of **12** with Me_4NOH in aq THF provided a 99% yield of di(carboxylic acid) **13**, which was converted into the corresponding di(acid chloride) by reaction with oxalyl chloride in C_6H_6. The crude di(acid chloride) was added to a mixture of NaH and dansylamide in THF to give ligand **2** in 75% yield.

Structures of new compounds **1**, **2**, **7**, **8** and **10**–**13** were verified by their ^1H NMR, ^{13}C NMR and IR spectra and by combustion analysis. The NMR spectra of new ionophores **1** and **2** showed that they are conformationally mobile.

Ligands **1** and **2** were converted into their di(tetraalkylammonium) salts **L1** and **L2**, respectively, by a reported method.[23]

2.2. Absorption spectra

Di-ionized ligand **L1** with two allyl groups on the upper rim exhibited an absorption band with a maximum at 327 nm in MeCN. The presence of 50 equiv of alkali metal cations (Li^+, Na^+, K^+, Rb^+, Cs^+) produced decreases in absorption intensity with red shifts, except with Cs^+ (Fig. 3a). For Cs^+, which is the largest alkali metal cation examined, enhanced absorption intensity with a red shift was observed. Di-ionized ligand **L2** with four allyl groups on the upper rim exhibited an absorption band with a maximum at 326 nm in MeCN (Fig. 4a). The presence of 50 equiv of alkali metal cations decreased the absorption intensity with red shifts. For **L2**, the effects of all five alkali metal cation species were all nearly the same. From comparison of the data presented in Figures 3a and 4a,

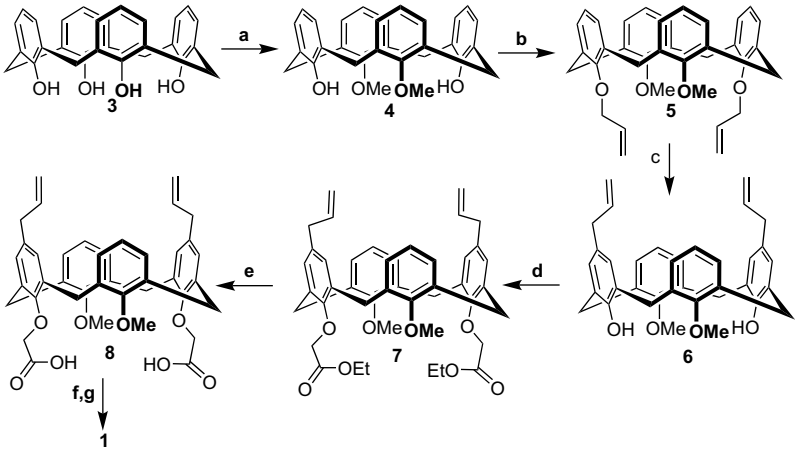

Scheme 1. Synthesis of didansyl di-ionizable calix[4]arene ionophore **1** with two upper-rim allyl groups: (a) MeOTs, K_2CO_3, MeCN, reflux, 20 h; (b) allyl bromide, NaH, THF, reflux, 15 h; (c) *N*,*N*-dimethylamiline, reflux, 2 h; (d) $BrCH_2CO_2Et$, NaH, THF, rt, 12 h; (e) 10% aq Me_4NOH, THF, rt, 12 h; (f) oxalyl chloride, C_6H_6, reflux, 5 h; (g) dansylamide, NaH, THF, rt, 12 h.

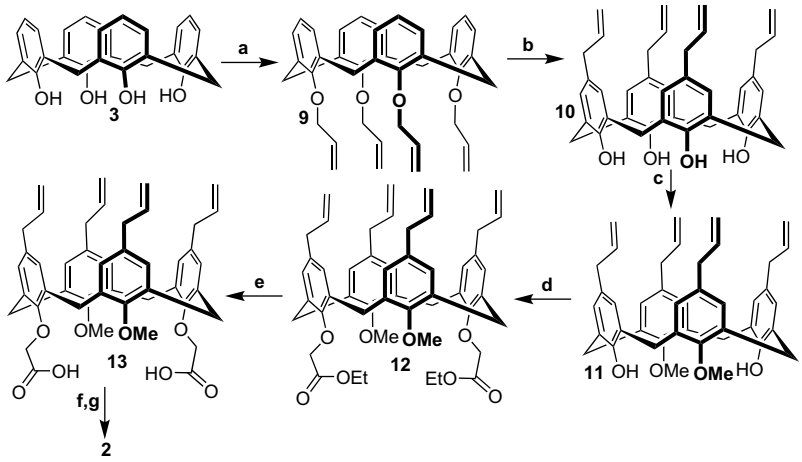

Scheme 2. Synthesis of didansyl, di-ionizable calix[4]arene ionophore **2** with four upper-rim allyl groups: (a) allyl bromide, NaH, THF/DMF (10:1), reflux, 2 h; (b) *N*,*N*-dimethylaniline, reflux, 2 h; (c) MeOTs, K_2CO_3, MeCN, reflux, 20 h; (d) $BrCH_2CO_2Et$, NaH, THF, rt 12 h; (e)10% aq Me_4NOH, THF, reflux, 12 h; (f) oxalyl chloride, C_6H_6, reflux, 12 h; (g) dansylamide, NaH, THF, rt, 12 h.

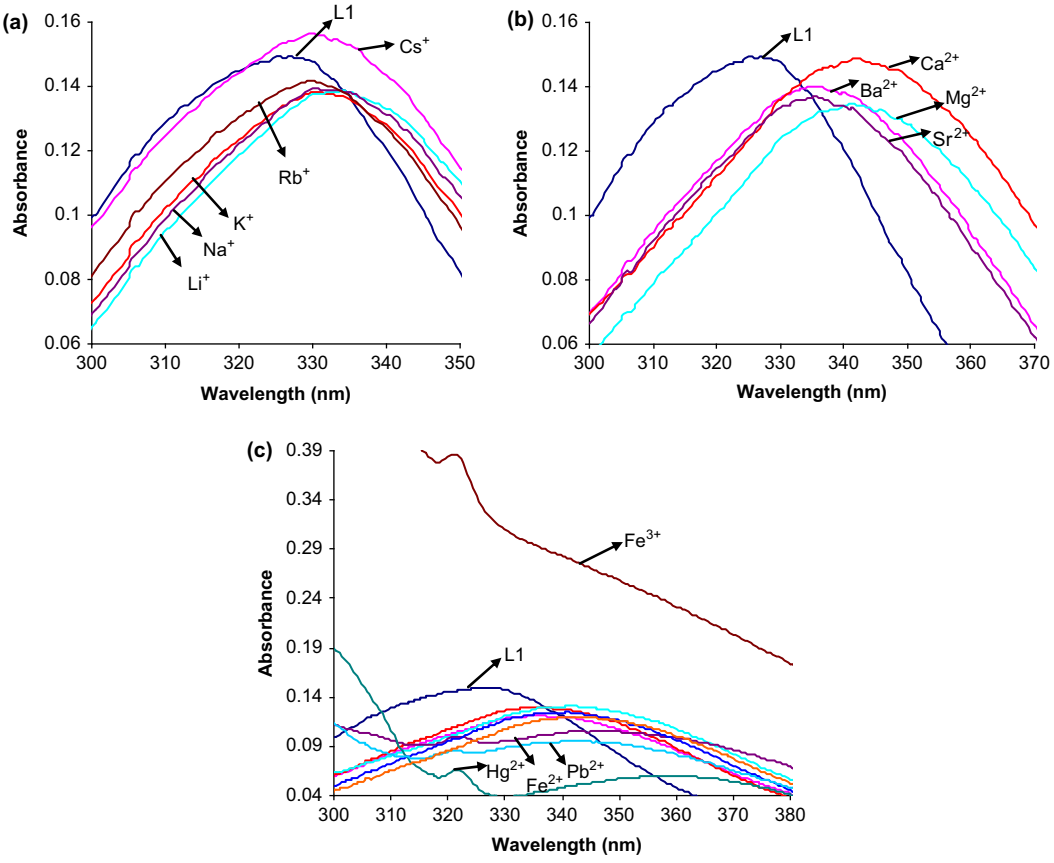

Figure 3. The effect of metal cations on the absorption spectra of **L1** in acetonitrile (a) for alkali metal cations; (b) for alkaline earth metal cations; (c) for transition metal cations and Pb^{2+}.

it is clear that the number of allyl groups on the upper rim influences the interaction of Cs^+ with the ligand.

Figure 3b shows the effect of 50 equiv of alkaline earth metal cations (Mg^{2+}, Ca^{2+}, Sr^{2+}, Ba^{2+}) on the absorption spectrum of **L1** in MeCN. The absorption band decreased in intensity with red shifts for all of the alkaline earth metal cations, except Ca^{2+}. In the presence of Ca^{2+} only a red shift of 15 nm was noted with little change in the absorption intensity. Mg^{2+} caused the same size of red shift with a decrease in absorption intensity. From comparison of the data shown in Figure 3a and b, it is evident that alkaline earth metal cations produced larger red shifts than alkali metal cations. The larger red shifts for alkaline earth metal cations result from their higher charge density. As seen in Figures 3b and 4b, increasing in the number of allyl groups affected the interaction of Ca^{2+} with the ligand. The presence of Ca^{2+} caused a pronounced absorption intensity decrease with a red shift when the number of upper-rim allyl groups was increased from two to four.

Figure 3c shows the effects of 50 equiv of transition metal cations (Ag^+, Cd^{2+}, Co^{2+}, Fe^{2+}, Hg^{2+}, Mn^{2+}, Zn^{2+}, Fe^{3+}) and Pb^{2+} on the absorption spectrum of **L1** in MeCN. Red shifts and absorption intensity decreases were observed with Ag^+, Cd^{2+}, Co^{2+}, Mn^{2+}, Pb^{2+} and Zn^{2+}. The effects of Hg^{2+} and Fe^{2+} on the absorption spectra of

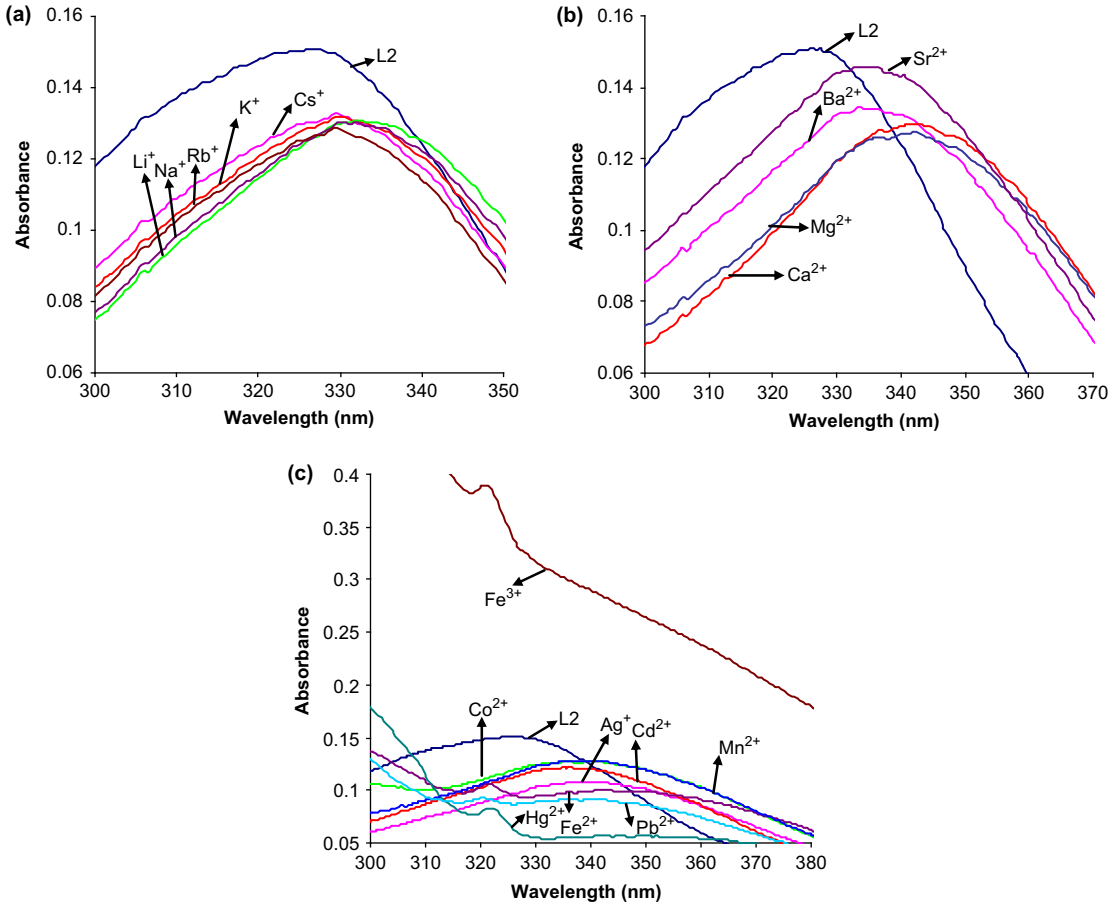

Figure 4. The effect of metal cations on the absorption spectra of **L2** in acetonitrile (a) for alkali metal cations; (b) for alkaline earth metal cations; (c) for transition metal cations and Pb^{2+}.

L1 were different from those of other transition metal cations in that they produced new absorption bands at about 323 nm. With Fe^{3+} there was a dramatic enhancement of absorption intensity which contrasts with the diminished absorptions observed for all of the other metal ion species examined. Comparison of the data in Figures 3c and 4c, reveals that transition metal cations and Pb^{2+} cation do not produce important changes in absorption spectra between 300 and 350 nm with variation of the number of upper-rim allyl groups from two to four.

2.3. Fluorescence spectra

When excited at 326 nm, ligands **L1** and **L2** gave emission bands with maxima at 470 and 471 nm, respectively, in MeCN. Figure 5 shows the effects of 50 equiv of metal cations on the fluorescence spectra of **L1**. As can be seen from Figure 5a, the emission band intensities were reduced somewhat in the presence of alkali metal cations with red shifts of the emission band from that of **L1**. The largest red shift and greatest quenching were produced by Li^{+}. Similar results were obtained for alkali metal cations with **L2** (Fig. 6a). Thus it was found that increasing the number of allyl groups on the upper rim from two to four did not change significantly the effect of alkali metal cations on the emission spectra.

The emission band intensity for **L1** was diminished substantially with red shifts for the alkaline earth metal cations (Fig. 5b). The effects of $Ba^{2+}$and Sr^{2+} and of Ca^{2+} and Mg^{2+} on the fluorescence spectra are nearly the same for each pair of metal ions. There are larger red shifts and greater quenching for Mg^{2+} and Ca^{2+}. For **L2** in the presence of alkaline earth metal cations, the effect was also substantial quenching with red shifts (Fig. 6b). In this case, the responses to Sr^{2+} and Ca^{2+} were similar. The quenching and red shift were greater for Ba^{2+}. The quenching effect of Mg^{2+} was even greater. The effects of transition metal cations and Pb^{2+} on the fluorescence spectra of **L1** and **L2** are presented in Figures 5c and 6c, respectively. Readily apparent is the strong to very strong quenching of the fluorescence of **L1** and **L2** in the presence of the transition metal cations and Pb^{2+}. With the exception of Ag^{+}, the responses of **L1** and **L2** to the presence of these metal ions are quite similar.

Magnitudes of the red shifts in the fluorescence emissions for **L**,[23] **L1** and **L2** are presented graphically in Figure 7. Note that structures for this ligand series are the same except for having no, two and four allyl groups attached to the upper rim, respectively. Except for Li^{+}, alkali metal cations caused red shifts of less than 20 nm with all of the ligands. Li^{+} produced appreciably larger red shifts among the alkali metal cations for all three ligands. The attachment of allyl groups to the upper rim of the ligand is seen to exert minor influence on the red shifts for the alkali metal cations. As can be seen in Figure 7, alkaline earth metal cations produce much larger red shifts with respect to alkali metal cations for all three ligands. Among the alkaline earth metal cations, the largest red shifts (52–63 nm) were found with Mg^{2+} and Ca^{2+}. The magnitudes of the red shifts are in the order **L**<**L1**<**L2**. For Sr^{2+} and Ba^{2+}, magnitudes of the red shifts decrease by about 20 nm with no clear effect of ligand structure. The effects of Mn^{2+} and Cd^{2+} on the red shift are in the order **L**>**L1**~**L2**. The greatest effect of allyl ligand structure on the red shift is observed for Fe^{2+}. The red shift increases by more than 40 nm in going from **L** to **L1**. Thus attaching two allyl groups to the upper rim of the ligand doubles the red shift from 46 nm to 87 nm. In view of this very

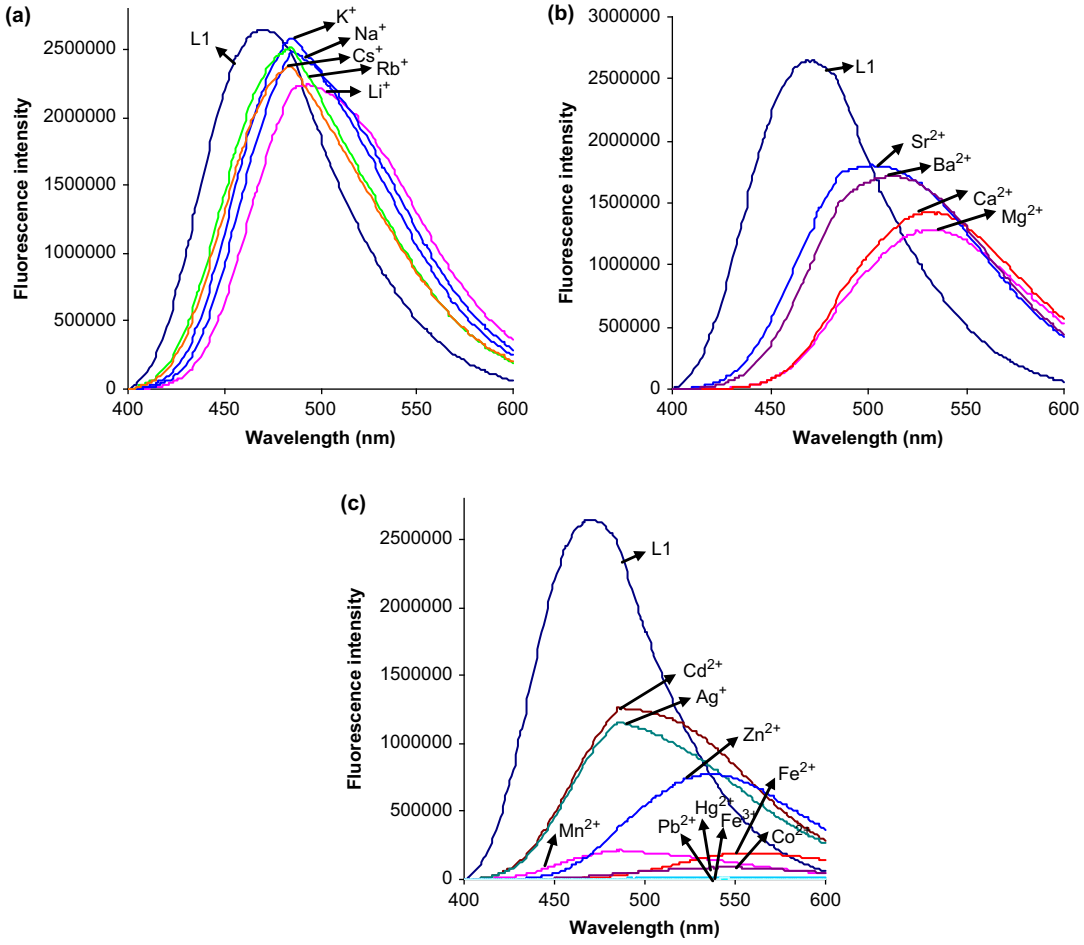

Figure 5. The effect of metal cations on the fluorescence spectra of **L1** in acetonitrile (a) for alkali metal cations; (b) for alkaline earth metal cations; (c) for transition metal cations and Pb^{2+}.

large change, it is surprising that increasing from two to four allyl groups has no significant effect on the magnitude of the red shift. It is interesting also that the interaction of Co^{2+} with **L** and **L2** produces red shifts of nearly 60 nm. On the other hand, interaction of Co^{2+} with **L1** increases the red shift by an additional 20 nm. Among the transition metal cations, Ag^{+} showed the smallest red shifts of about 20 nm for all three ligands. Magnitudes of the red shifts for **L**, **L1** and **L2** are all in the range of 60–70 nm for Zn^{2+}.

Figure 8 presents the relative changes of fluorescence intensity at the wavelength of maximum emission for ligands **L**,[23] **L1** and **L2**. Quenching is observed in the presence of alkali metal cations for all three ligands, except for Rb^{+} with **L2**. The greatest quenching is observed for Li^{+} among alkali metal cations for the three ligands. However, the magnitude of the quenching (below 20%, but mostly under 10%) is relatively small with all of the alkali metal cations. Alkaline earth metal cations cause greater quenching than alkali metal cations. It is interesting that there are regular increases (albeit usually small) in the quenching efficiency with Mg^{2+}, Sr^{2+} and $Ba^{2+}$when the ligand was changed from **L** to **L1** and **L2**. Similar effects are noted for Co^{2+} and Ag^{+}, but with a significant increase in quenching efficiency for **L2** with four allyl groups on the upper rim. The situation is just the opposite with Cd^{2+}, for which **L** exhibits the greatest quenching. Pb^{2+} and transition metal cations of Co^{2+}, Fe^{2+}, Hg^{2+}, Mn^{2+} and Fe^{3+} produce strong fluorescence quenching (>90%) for all three ligands. The presence of Fe^{3+}, Pb^{2+} and Hg^{2+} gave greater than 99% quenching of the dansyl fluorescence for ligands **L**, **L1** and **L2**.

2.4. Determination of stability constants

Stability constants and stoichiometries for complexation of Hg^{2+}, Pb^{2+} and Fe^{3+} by ligands **L1** and **L2** in MeCN were determined by spectrofluorimetric titration. The ligand concentration was held constant at 2.58×10^{-5} M. Stoichiometries of the complexes and their stability constants were determined from changes in the fluorescence intensity as a function of the metal ion concentration. Successive decreases of emission with increases in the metal ion concentration were observed in all of the fluorimetric titrations.

Figure 9 shows the fluorescence spectra of **L2** in MeCN with increasing concentrations of Hg^{2+}. The inserts in Figure 9 are a plot of the change of fluorescence intensity versus the ratio of [metal ion]/[ligand] and a plot of the quantity $I_0/(I_0-I)$ versus [metal ion]$^{-1}$. The break in the former at [metal ion]/[ligand]=1.0 provides strong evidence for formation of a 1:1 complex. Similar plots were found with Pb^{2+} for **L1** and **L2** in MeCN. However, Fe^{3+} gave a 1:2 (M/L) complex with both ligands (Table 1). Also, Hg^{2+} gave a 1:2 (M/L) complex with **L1**. The stability constant for a complex is obtained from a plot of the quantity $I_0/(I_0-I)$ versus [metal ion]$^{-1}$. The ratio of intercept/slope gives the stability constant.[24]

Table 1 presents stability constants and complex stochiometries for complexation of with Fe^{3+}, Hg^{2+} and Pb^{2+} by **L**,[23] **L1** and **L2**. The log β values vary between 3.10 and 5.40 and show that the ionized ligands interact strongly with these metal ions in MeCN. For 1:1 complexation of Pb^{2+} by the three ligands, the

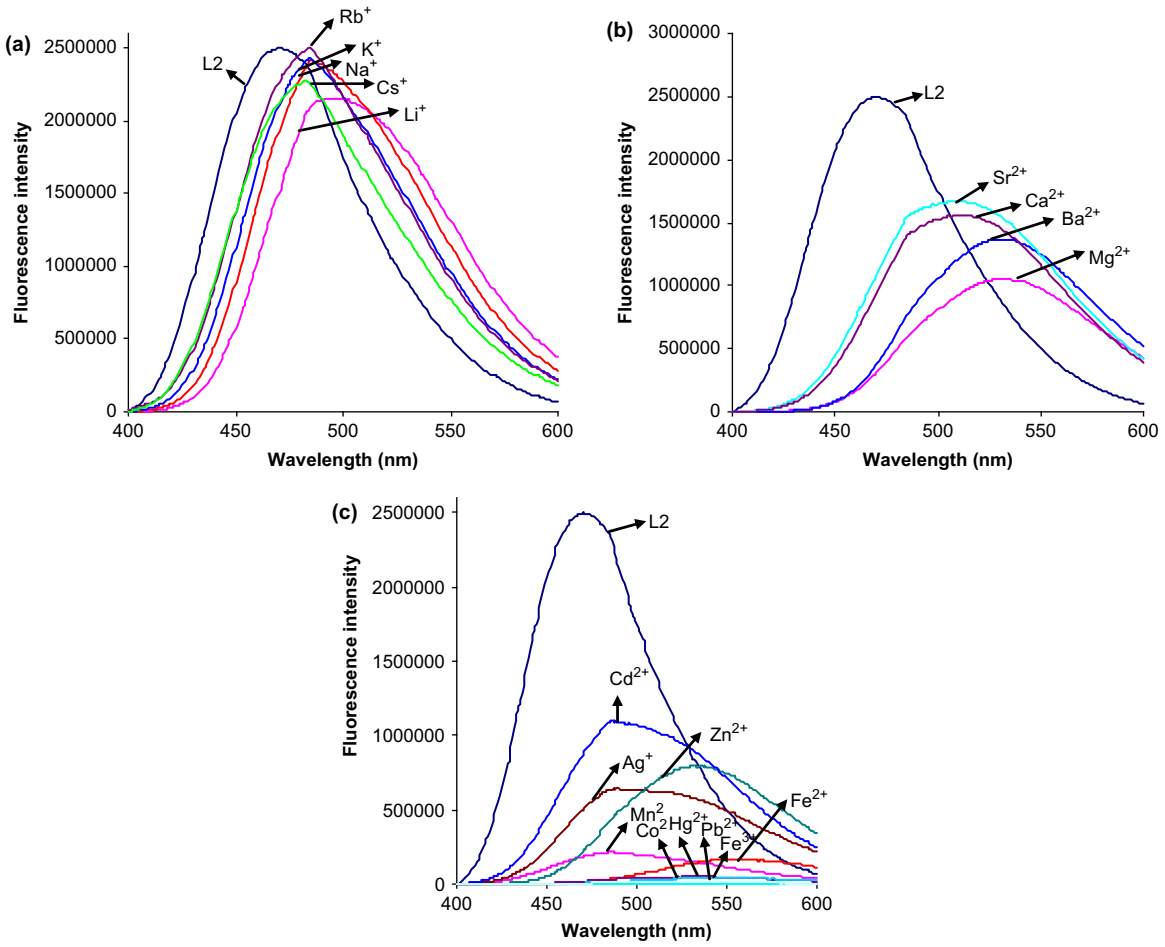

Figure 6. The effect of metal cations on the fluorescence spectra of **L2** in acetonitrile (a) for alkali metal cations; (b) for alkaline earth metal cations; (c) for transition metal cations and Pb^{2+}.

stability constants decrease in the order: **L**>**L2**>**L1**. Thus, the attachment of either two or four allyl groups to the upper rim of di-ionized ligand **L** diminishes the propensity for complexation of Pb^{2+} in MeCN. A similar result was obtained for Pb^{2+} complexation by the upper-rim *tert*-butyl-substituted ligand series shown in Figure 1.[23]

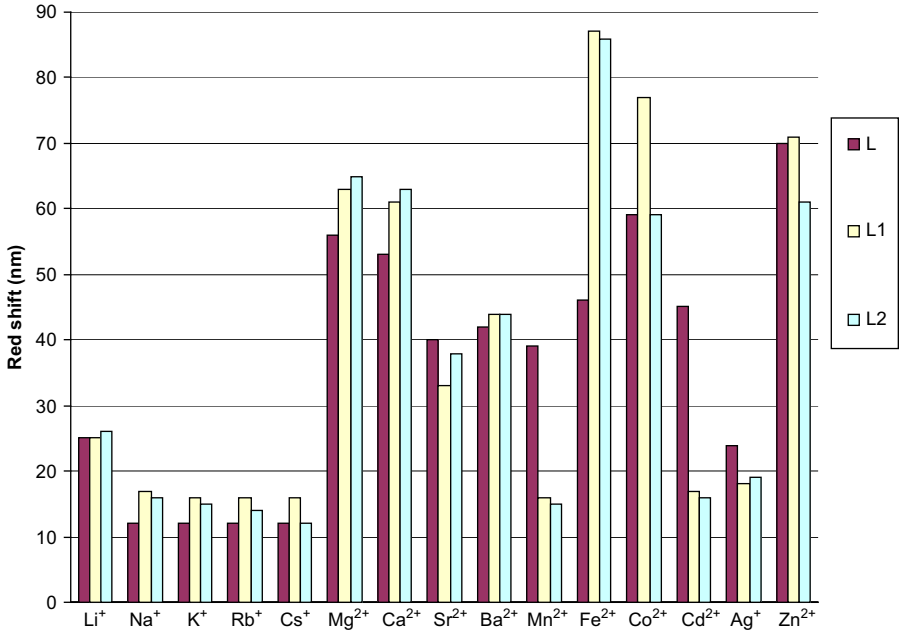

Figure 7. Bar chart of the red shift in the fluorescence emission observed at the wavelength of maximum emission for different metal ions with **L**, **L1** and **L2**.

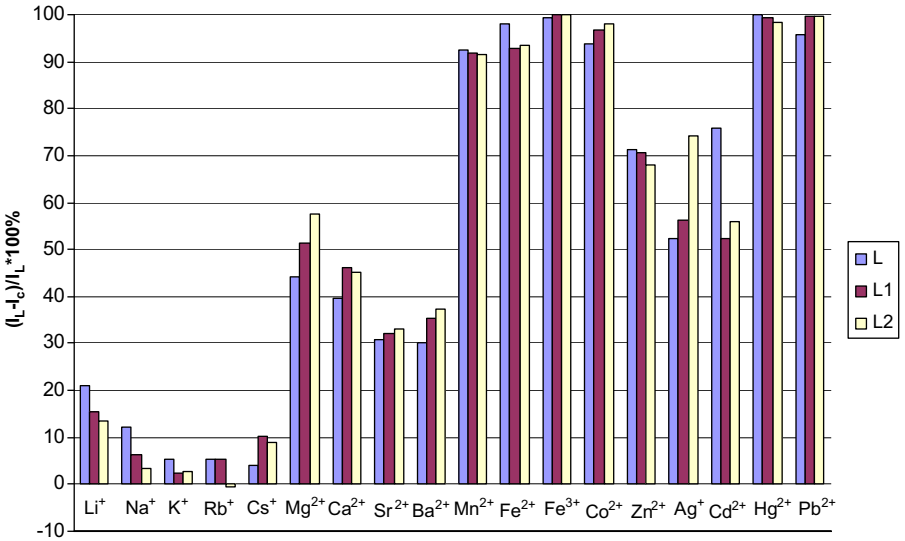

Figure 8. Bar chart of quenching efficiency for different metal ions observed at the wavelength of maximum emission for **L**, **L1** and **L2**.

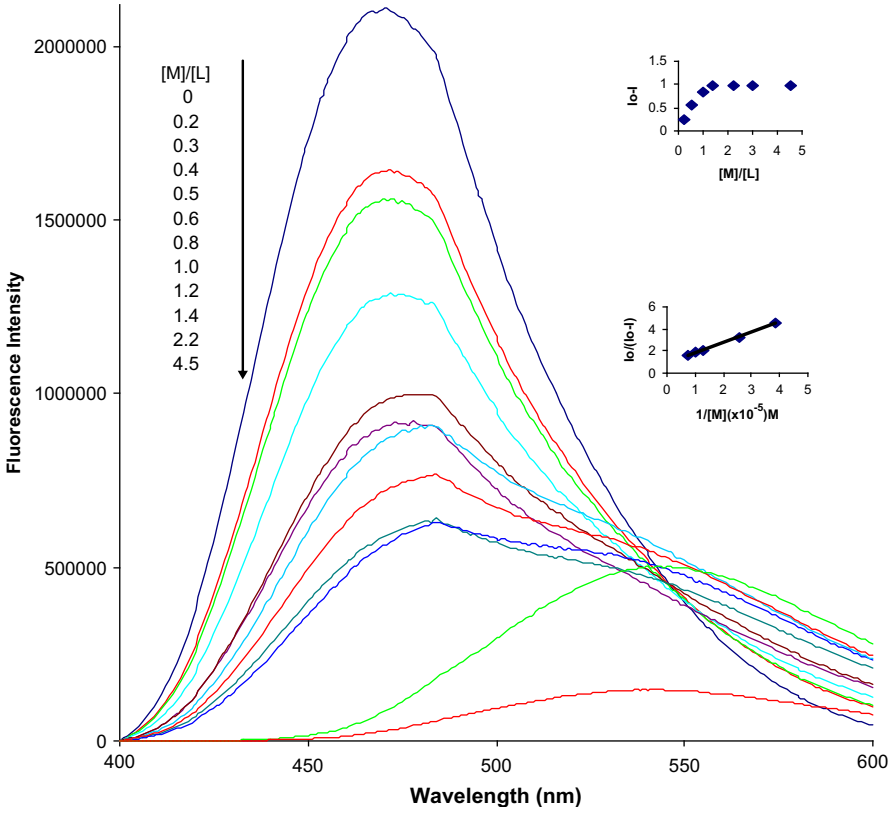

Figure 9. Fluorescence spectra (λ_{exc}=326 nm) of **L2** in MeCN with increasing amounts of Hg^{2+}. [L]: 2.58×10^{-5} M (For identification of insets, see the text.).

Table 1
Stability constants and stoichiometries for complexation of **L**, **L1** and **L2** with Hg^{2+}, Pb^{2+} and Fe^{3+} in MeCN

Ionized ligand	Stability constant (log β) Cation			Complex stochiometry (M/L) Cation		
	Fe^{3+}	Pb^{2+}	Hg^{2+}	Fe^{3+}	Pb^{2+}	Hg^{2+}
L	3.94±0.02[a]	4.76±0.04[a]	4.53±0.03[a]	1:1[a]	1:1[a]	1:1[a]
L1	5.34±0.01	3.10±0.03	5.16±0.03	1:2	1:1	1:2
L2	5.40±0.02	3.27±0.05	4.91±0.02	1:2	1:1	1:1

[a] Ref. 23.

In contrast with the results obtained earlier with the ligand series shown in Figure 1 for which only 1:1 complexes were formed with these three metal ion species, 1:2 (M/L) complexes are observed between Fe^{3+} and either **L1** or **L2** and between Hg^{2+} and **L1**. This change in stoichiometry suggests possible interaction of the second ligand molecule via one of the upper-rim allyl groups.

2.5. Stern–Volmer analysis

Stern–Volmer analysis was utilized to probe the nature of the quenching process in the complexation of Fe^{3+}, Hg^{2+} and Pb^{2+}.

Stern–Volmer plots are a useful method of presenting data on emission quenching.[25,26] Plotting relative emission intensities (I_0/I) against quencher concentration [Q] yields a linear Stern–Volmer plot for a static quenching process. Expressed as Eq. 1, the slope of this line is Ksv, the static quenching constant. I and I_0 are fluorescence intensities in the presence and in the absence of added metal cations.

$$I_0/I = 1 + \mathrm{Ksv}[Q] \quad (1)$$

Figure 10 shows the steady-state emission Stern–Volmer analysis for complexation of Hg^{2+} by **L2**. For both **L1** and **L2**, linear behavior was observed for complexation of Fe^{3+}, Hg^{2+} and Pb^{2+}. These results are consistent with static quenching.

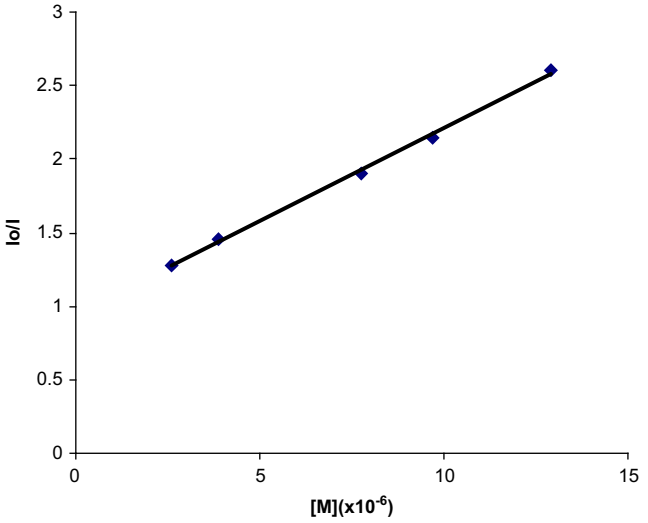

Figure 10. Stern–Volmer plot for the fluorescence quenching of **L2** by Hg^{2+} in MeCN.

2.6. Summary

This study probes the influence of a systematic structural variation within calix[4]arene ligands having two ionized, dansyl-containing side arms on the lower rim upon their spectroscopic responses to metal ions. The upper rim is modified to possess zero, two and four allyl groups. In the presence of excess metal ions in MeCN, fluorescence quenching increases in the order: alkali metal cations<alkaline earth metal cations<transition and heavy metal cations. The presence of Fe^{3+}, Pb^{2+} and Hg^{2+} gave greater than 99% quenching of the dansyl fluorescence for the three ligands. For the ligand with no allyl groups on the upper rim, only 1:1 (M/L) complexes are formed with all three of these metal ion species. For the ligand with two allyl groups on the upper rim, 1:2 (M/L) complexes were found with Fe^{3+} and Hg^{2+} suggesting that the metal ion complexed by one ligand molecule is associating with the π bond on the upper rim of a second ligand molecule. Information gained from this study is important in evaluating the potential for such di-ionized, dansyl-containing ligands in fluorogenic metal ion sensors.

3. Experimental

3.1. General

The ^1H and ^{13}C NMR spectra were recorded with Varian Unity INOVA 500 MHz FT-NMR (^1H at 500 MHz and ^{13}C at 126 MHz) spectrometer in $CDCl_3$ with Me_4Si as internal standard. Chemical shifts (δ) are given in parts per million downfield from TMS and coupling constant (J) values are in hertz. IR spectra were recorded with a Perkin–Elmer model 1600 FT-IR spectrophotometer as deposits from $CDCl_3$ solutions on a NaCl plate. Absorption spectra were recorded with a Shimadzu model 2401PC UV–visible spectrophotometer. Fluorescence spectra were obtained with a SLM Aminco 8000C photon counting spectrofluorometer equipped with a 450-W ozone-free xenon lamp as the light source. Elemental analysis was performed by Desert Analytics Laboratory of Tucson, Arizona.

Reagents were obtained from commercial suppliers and used directly unless otherwise noted. Tetrahydrofuran (THF) was dried over sodium with benzophenone as an indicator and distilled just before use. Spectrometric grade acetonitrile (MeCN) from EM was the solvent for absorption and fluorescence measurements. All metal perchlorates purchased from Acros were of the highest available quality and vacuum dried over blue silica gel before use.

The 25,27-dihydroxy-26,28-dimethoxycalix[4]arene (**4**),[27] 25,27-diallyloxy-26,28-dimethoxycalix[4]arene (**5**),[27] 11,23-diallyl-25,27-dihydroxy-26,28-dimethoxycalix[4]arene (**6**),[27] 25,26,27,28-tetraallyloxycalix[4]arene (**9**)[28] and 5,11,17,23-tetraallyl-25,26,27,28-tetra-hydroxycalix[4]arene (**10**)[28] were prepared by the reported procedures.

3.2. Absorption and fluorescence measurements

Absorption spectra of the di-ionized ligands (2.58×10^{-5} M) in MeCN solutions containing 50 mol equiv of the appropriate metal perchlorate salt were measured using a 1 cm absorption cell. Fluorescence spectra of the same solutions were measured with a 1 cm quartz cell. The excitation wavelength was 326 nm for all of the ionized ligands. Fluorescence emission spectra were recorded in the range 400–750 nm with a slit width of 1.0 nm.

The stoichiometries of the complexes and their stability constants were determined according to a literature procedure.[24]

3.3. Ligand synthesis

*3.3.1. 11,23-Diallyl-25,27-bis(ethoxycarbonylmethoxy)-26,28-dimethoxycalix[4]arene (**7**)*

A mixture of **6**[27] (2.00 g, 3.75 mmol) and NaH (0.36 g, 15.00 mmol) in 50 ml of THF was stirred under nitrogen at room temperature for 30 min. Ethyl bromoacetate (3.77 g, 12.50 mmol) in THF (50 mL) was added slowly. The mixture was stirred at room temperature for another 12 h and quenched with a small amount of water added dropwise. The THF was evaporated in vacuo. CH_2Cl_2 (100 mL) and 10% HCl (50 mL) were added to the residue. The organic layer was separated, washed with water (2×50 ml), dried over $MgSO_4$ and evaporated in vacuo. Crystallization of the residue from MeOH gave 2.32 g (88%) of diester **7** as a white solid with mp 139 °C. IR (deposit from $CDCl_3$ solution onto a NaCl plate): 2730 (CH=CH_2), 1764 (C=O), 1199 (C–O) cm^{-1}. ^1H NMR ($CDCl_3$) δ 7.34 (s, 1H), 7.11 (d, J=7.4 Hz, 2H), 7.06 (s, 1H), 6.92 (t, J=7.3 Hz, 2H), 6.76 (s, 1H), 6.22 (s, 1H), 6.13 (s, 2H), 5.79–5.70 (m, 1H), 5.57–5.49 (m, 1H), 4.95 (d, J=9.9 Hz, 1H), 4.89 (d, J=17.0 Hz, 1H), 4.78 (d, J=9.9 Hz, 1H), 4.65 (d, J=17.0 Hz, 1H), 4.41–4.38 (m, 4H), 4.30–4.24 (m, 4H), 4.03 (s, 4H), 3.84–3.48 (m, 4H), 3.83–3.48 (m, 4H), 3.17 (d, J=13.2 Hz, 2H), 3.03 (d, J=6.2 Hz, 2H), 2.77 (d, J=6.3 Hz, 2H), 1.31 (t, J=7.2 Hz, 6H); ^{13}C NMR δ 169.4, 158.9, 158.1, 154.3, 153.5, 138.0, 137.8, 136.6, 133.8, 133.4, 132.9, 128.7, 127.7, 122.5, 114.9, 114.7, 72.1, 71.1, 60.9, 60.8, 39.3, 39.1, 30.8, 14.2. Anal. Calcd for $C_{44}H_{48}O_8$: C, 74.98; H, 6.86. Found: C, 74.59; H, 6.98.

*3.3.2. 11,23-Diallyl-25,27-bis(carbonylmethoxy)-26,28-dimethoxycalix[4]arene (**8**)*

A mixture of **7** (2.00 g, 2.84 mmol), THF (50 mL) and 10% aq Me_4NOH (50 mL) was refluxed for 12 h. The THF was evaporated in

vacuo and the resulting aq mixture was cooled in an ice-bath and acidified with 6 N HCl. The mixture was extracted with CH_2Cl_2 (2×100 mL). The combined organic layers were washed with water (2×50 ml) and dried over $MgSO_4$. After evaporation of the THF in vacuo, diacid **8** (1.90 g, 99%) was obtained as a white solid with mp 233 °C. IR (deposit from $CDCl_3$ solution onto a NaCl plate): 3180 (br, O–H), 2800 (CH═CH_2), 1757 (C═O), 1214 (C–O) cm^{-1}. ^1H NMR ($CDCl_3$) δ 6.99 (s, 4H), 6.59–6.55 (m, 6H), 6.02–5.94 (m, 2H), 5.11–5.03 (m, 4H), 4.68 (s, 4H), 4.25 (d, J=13.2 Hz, 4H), 3.83 (s, 6H), 3.36 (d, J=6.6 Hz, 4H), 3.32 (d, J=15.9 Hz, 4H); ^{13}C NMR δ 169.7, 154.0, 153.0, 137.3, 136.4, 134.8, 132.6, 129.5, 128.7, 124.4, 116.0, 72.1, 63.8, 39.4, 30.7. Anal. Calcd for $C_{40}H_{40}O_8$: C, 74.06; H, 6.22. Found: C, 73.93; H, 6.04.

3.3.3. *11,23-Diallyl-25,27-bis[N-(dansylsulfonyl) carbamoylmethoxy]-26,28-dimethoxycalix[4]arene (**1**)*

A solution of **8** (0.98 g, 1.51 mmol) and oxalyl chloride (1.57 g, 12.4 mmol) in benzene (60 mL) was refluxed for 5 h. The solution was evaporated in vacuo and dried under high vacuum for 30 min. The residue was dissolved in THF (20 mL) and the solution was added to a mixture of dansylamide (0.95 g, 3.78 mmol) and NaH (0.36 g, 15.10 mmol) in THF (40 mL) under nitrogen at room temperature. The reaction mixture was stirred for another 12 h. The reaction was quenched with a small amount of water and the THF was evaporated in vacuo. The residue was dissolved in CH_2Cl_2 (100 mL) and washed with 10% aq K_2CO_3 solution (2×50 mL), 10% HCl (50 mL) and water (2×50 mL). The organic layer was dried over $MgSO_4$ and evaporated in vacuo to give the crude product, which was chromatographed on silica gel with EtOAc/hexanes (1:1) as eluent to produce 3.87 g (76%) of a light yellow solid with mp 208–210 °C. IR (deposit from $CDCl_3$ solution onto a NaCl plate): 3344 (br, N–H), 2824 (CH═CH_2), 1733 (C═O), 1213, 1140 (C–O) cm^{-1}. ^1H NMR ($CDCl_3$) δ 9.54 (br s, 2H), 8.65–8.62 (m, 4H), 8.54 (d, J=8.5 Hz, 2H), 7.79–7.75 (m, 2H), 7.60 (t, J=8.1 Hz, 2H), 7.22 (d, J=6.2 Hz, 2H), 7.10–6.40 (m, 8H), 5.82–5.78 (m, 2H), 4.98 (d, J=10.0 Hz, 2H), 4.83 (d, J=16.1 Hz, 2H), 3.80–2.80 (m, 34H); ^{13}C NMR δ 167.0, 158.4, 152.1, 151.7, 137.6, 135.0, 134.3, 133.3, 132.9, 131.7, 129.9, 129.8, 129.7, 129.1, 123.5, 118.7, 115.4, 71.6, 45.4, 39.1. Anal. Calcd for $C_{64}H_{64}O_{10}N_4S_2$: C, 69.04; H, 5.79, N, 5.03. Found: C, 68.88; H, 5.95, N, 4.95.

3.3.4. *5,11,17,23-Tetraallyl-25,27-dihydroxy-26,28-dimethoxycalix[4]arene (**11**)*

A solution of **10**[28] (1.30 g, 2.22 mmol) and K_2CO_3 (0.34 g, 2.44 mmol) in 25 mL of MeCN was refluxed for 30 min. A solution of MeOTs (0.46 g, 2.44 mmol) in 8 ml of MeCN was added dropwise over a period of 30 min. After refluxing for 10 h, additional MeOTs (0.46 g, 2.44 mmol) in 8 ml of MeCN was added and the reaction mixture was refluxed for another 10 h. The solvent was removed in vacuo and the residue was dissolved in 100 mL of CH_2Cl_2. After acidification with concd HCl to pH=1, the mixture was washed with 1 N HCl (50 mL) and then water (50 mL). The organic layer was dried over $MgSO_4$ and evaporated in vacuo. Recrystallization of the residue from isopropyl alcohol gave 1.25 g (90%) of **11** as a white solid with mp 146–147 °C. IR (deposit from $CDCl_3$ solution onto a NaCl plate): 3354 (br, O–H), 2831 (CH═CH_2), 1228 (C–O) cm^{-1}. ^1H NMR ($CDCl_3$) δ 7.83 (s, 2H), 6.86 (s, 4H), 6.71 (s, 4H), 6.00–5.91 (m, 2H), 5.82–5.73 (m, 2H), 5.06–4.86 (m, 8H), 4.26 (d, J=13.0 Hz, 4H), 3.96 (s, 6H), 3.33 (d, J=13.0 Hz, 4H), 3.26 (d, J=6.6 Hz, 4H), 3.08 (d, J=6.6 Hz, 4H); ^{13}C NMR δ 151.7, 151.2, 138.3, 137.4, 136.3, 133.1, 130.3, 129.1, 128.6, 128.2, 115.5, 115.1, 63.5, 39.5, 39.4, 31.3. Anal. Calcd for $C_{42}H_{44}O_4$: C, 82.37; H, 7.18. Found: C, 82.76; H, 6.96.

3.3.5. *5,11,17,23-Tetraallyl-25,27-di(ethoxycarbonylmethoxy)-26,28-dimethoxycalix[4]arene (**12**)*

A mixture of **11** (2.00 g, 3.27 mmol) and NaH (0.31 g, 12.92 mmol) in 50 mL of THF was stirred under nitrogen at room temperature for 30 min. Ethyl bromoacetate (3.28 g, 19.62 mmol) in THF (50 mL) was added slowly. The mixture was stirred at room temperature for another 12 h and quenched with a small amount of water (added dropwise). The THF was evaporated in vacuo. CH_2Cl_2 (100 mL) and 10% HCl (50 mL) were added to the residue. The organic layer was washed with water (2×50 mL), dried over $MgSO_4$ and evaporated in vacuo. Crystallization of the residue from MeOH gave 2.00 g (78%) of diester **12** as a white solid with mp 75 °C. IR (deposit from $CDCl_3$ solution onto a NaCl plate): 2831 (CH═CH_2), 1763 (C═O), 1189 (C–O) cm^{-1}. ^1H NMR ($CDCl_3$) δ 7.16 (s, 1H), 6.94 (s, 2H), 6.89 (s, 1H), 6.75 (s, 1H), 6.24 (s, 1H), 6.14 (s, 2H), 6.10–6.00 (m, 2H), 5.80–5.71 (m, 1H), 5.57–5.48 (m, 1H), 5.20–5.02 (m, 4H), 4.97–4.89 (m, 2H), 4.81 (d, J=9.9 Hz, 1H), 4.80 (d, J=17.1 Hz, 1H), 4.51–4.14 (m, 10H), 4.00 (s, 4H), 3.80–3.00 (m, 14H), 2.80 (d, J=6.3 Hz, 2H), 1.31 (m, 6H); ^{13}C NMR δ 169.2, 169.5, 157.1, 156.3, 154.3, 153.5, 138.4, 138.0, 137.7, 136.4, 133.7, 133.6, 133.4, 132.8, 129.0, 127.6, 115.1, 114.9, 114.8, 72.1, 71.0, 60.9, 60.8, 39.6, 39.3, 39.1, 30.8, 14.2. Anal. Calcd for $C_{50}H_{56}O_8 \cdot 0.6MeOH$: C, 75.69; H, 7.18. Found: C, 75.55; H, 7.08.

3.3.6. *5,11,17,23-Tetraallyl-25,27-bis(carbonylmethoxy)-26,28-dimethoxycalix[4]arene (**13**)*

A mixture of **12** (9.90 g, 12.61 mmol), THF (250 mL) and 10% aq Me_4NOH (250 mL) was refluxed for 12 h. The THF was evaporated in vacuo and the resulting aq mixture was cooled in an ice-bath and acidified with 6 N HCl. The mixture was extracted with CH_2Cl_2 (2×100 mL). The combined organic layers were washed with water (2×50 mL) and dried over $MgSO_4$. After evaporation of the THF in vacuo, diacid **13** (9.10 g, 99%) was obtained as a white solid with mp 131 °C. IR (deposit from $CDCl_3$ solution onto a NaCl plate): 3189 (br, OH), 2825 (CH═CH_2), 1760 (C═O), 1224 (C–O) cm^{-1}. ^1H NMR ($CDCl_3$) δ 11.40 (br, 2H), 6.98 (s, 4H), 6.36 (s, 4H), 6.03–5.95 (m, 2H), 5.56–5.48 (m, 2H), 5.09–5.06 (dq, J=10.1, 1.7 Hz, 2H), 4.98–4.94 (dq, J=17.1, 1.8 Hz, 2H), 4.83–4.79 (dq, J=10.1, 1.7 Hz, 2H), 4.67 (s, 4H), 4.61–4.56 (dq, J=17.2, 1.8 Hz, 2H), 4.2 (d, J=13.1 Hz, 4H), 3.81 (s, 6H), 3.34 (d, J=6.1 Hz, 4H), 3.29 (d, J=13.2 Hz, 4H), 2.86 (d, J=6.3 Hz, 4H); ^{13}C NMR δ 169.6, 153.9, 151.3, 37.7, 136.9, 136.3, 135.3, 134.8, 132.4, 129.7, 128.8, 115.7, 115.3, 72.1, 63.8, 39.3, 39.0, 30.7. Anal. Calcd for $C_{46}H_{48}O_8$: C, 75.80; H, 6.64. Found: C, 76.18; H, 6.38.

3.3.7. *5,11,17,23-Tetraallyl-25,27-bis[N-(dansylsulfonyl) carbamoylmethoxy]-26,28-dimethoxycalix[4]arene (**2**)*

Use of the procedure given above for conversion of diacid **8** into ligand **1**, but replacing **8** with diacid **13**, gave a 74% yield of ligand **2** as light yellow solid with mp 149–150 °C. IR (deposit from $CDCl_3$ solution onto a NaCl plate): 3352 (br, N–H), 2780 (CH═CH_2), 1742 (C═O), 1212, 1140 (C–O) cm^{-1}. ^1H NMR ($CDCl_3$) δ 9.76 (br, 2H), 8.80–8.40 (m, 6H), 8.00–7.20 (m, 6H), 6.85 (s, 4H), 6.67 (s, 4H), 6.10–5.40 (m, 4H), 5.18–4.70 (m, 8H), 4.25–4.00 (m, 4H), 3.80–3.45 (m, 8H), 3.45–2.55 (m, 26H); ^{13}C NMR δ 167.9, 156.7, 151.9, 138.0, 137.7, 134.9, 134.2, 133.6, 133.1, 131.3, 129.8, 129.7, 128.8, 124.2, 115.4, 115.2, 71.2, 58.0, 45.7, 39.0, 38.7, 37.4. Anal. Calcd for $C_{70}H_{72}O_{10}N_4S_2 \cdot 0.5CH_2Cl_2$: C, 68.51; H, 5.95, N, 4.53. Found: C, 68.70; H, 5.91, N, 4.16.

3.3.8. *Preparation of the di(tetramethylammonium) salts of the di-ionized ligands*

Di(tetramethylammonium) salts of ligands **1** and **2** (**L1** and **L2**, respectively) were prepared according to a published procedure.[23]

Acknowledgements

This work was supported by The Scientific and Technological Research Council of Turkey (TUBITAK). We also thank the Division of Chemical Sciences, Geosciences and Biosciences of the Office of Basic Energy Sciences of the U.S. Department of Energy (Grant DE-FG02-90ER14416) for support of this research.

References and notes

1. Valeur, B.; Leray, I. *Coord. Chem. Rev.* **2000**, *205*, 3–40.
2. Mancin, F.; Rampazzo, E.; Tecilla, P.; Tonellato, U. *Chem.—Eur. J.* **2006**, *12*, 1844–1854.
3. Wang, M. X.; Meng, X. M.; Zhu, M. Z.; Guo, Q. X. *Chin. Chem. Lett.* **2008**, *19*, 977–980.
4. Klonkowski, A. M.; Kledzik, K.; Ostaszewski, R. *J. Inclusion Phenom. Macrocycl. Chem.* **1999**, *35*, 165–171.
5. Yoon, S.; Miller, E. W.; He, Q.; Do, P. H.; Chang, C. J. *Angew. Chem., Int. Ed.* **2007**, *46*, 6658–6661.
6. Ludwig, R.; Dzung, N. T. K. *Sensors* **2002**, *2*, 397–416.
7. Kim, S. K.; Kim, S. H.; Kim, H. J.; Lee, S. H.; Lee, S. W.; Ko, J.; Bartsch, R. A.; Kim, J. S. *Inorg. Chem.* **2005**, *44*, 7866–7875.
8. Souchon, V.; Leray, I.; Valeur, B. *Chem. Commun.* **2006**, 4224–4226.
9. Quang, D. T.; Jung, H. S.; Yoon, J. H.; Lee, S. Y.; Kim, J. S. *Bull. Korean Chem. Soc.* **2007**, *28*, 682–684.
10. Liu, H.; Xu, Y.; Li, B.; Yin, G.; Xu, Z. *Chem. Phys. Lett.* **2001**, *345*, 395–399.
11. Kim, S. K.; Lee, J. K.; Lim, J. M.; Kim, J. W.; Kim, J. S. *Bull. Korean Chem. Soc.* **2004**, *25*, 1247–1250.
12. Osipov, M.; Chu, Q.; Geib, S. J.; Curran, D. P.; Weber, S. G. *Beilstein J. Org. Chem.* **2008**, *4*, 36.
13. Leray, I.; Lefevre, J. P.; Delouis, J. F.; Delaire, J.; Valeur, B. *Chem.—Eur. J.* **2001**, *7*, 4590–4598.
14. Agrawal, Y. K.; Pancholi, J. P. *Synth. Commun.* **2008**, *38*, 2446–2458.
15. Sessler, J. L.; Kim, S. K.; Gross, D. E.; Lee, C. H.; Kim, J. S.; Lynch, V. M. *J. Am. Chem. Soc.* **2008**, *130*, 13162–13166.
16. Chen, Q. Y.; Chen, C. F. *Tetrahedron Lett.* **2005**, *46*, 165–168.
17. Li, G. K.; Liu, M.; Yang, G. Q.; Chen, C. F.; Huang, Z. T. *Chin. J. Chem.* **2008**, *26*, 1440–1446.
18. Metivier, R.; Leray, I.; Valeur, B. *Chem. Commun.* **2003**, 996–997.
19. Jose, P.; Menon, S. *Bioinorg. Chem. Appl.* **2007**, Article ID 65815.
20. Talanova, G. G.; Roper, E. D.; Buie, N. M.; Gorbunova, M. G.; Bartsch, R. A.; Talanov, V. S. *Chem. Commun.* **2005**, 5673–5675.
21. Tu, C.; Surowiec, K.; Gega, J.; Purkiss, D. W.; Bartsch, R. A. *Tetrahedron* **2008**, *64*, 1187–1196.
22. Tu, C.; Surowiec, K.; Bartsch, R. A. *Tetrahedron* **2007**, *63*, 4184–4189.
23. Ocak, Ü.; Ocak, M.; Surowiec, K.; Bartsch, R. A.; Gorbunova, M. G.; Tu, C.; Surowiec, M. A. *J. Inclusion Phenom. Macrocycl. Chem.* **2009**, *63*, 131–139.
24. Bourson, J.; Valeur, B. *J. Phys. Chem.* **1989**, *93*, 3871–3876.
25. Murphy, C. B.; Zhang, Y.; Troxler, T.; Ferry, V.; Martin, J. J.; Jones, W. E. *J. Phys. Chem. B* **2004**, *108*, 1537–1543.
26. Larsen, R. W.; Helms, M. K.; Everett, W. R.; Jameson, D. M. *Photochem. Photobiol.* **1999**, *69*, 429–434.
27. von Loon, J. D.; Arduini, A.; Coppi, L.; Verboom, W.; Pochini, A.; Ungaro, R.; Harkema, S.; Reinhoudt, D. N. *J. Org. Chem.* **1990**, *55*, 5639–5646.
28. Gutsche, C. D.; Levine, J. A.; Sujeeth, P. H. *J. Org. Chem.* **1985**, *50*, 5802–5806.